Biomaterials 62 (2015) 138–146

Contents lists available at ScienceDirect

Biomaterials

journal homepage: www.elsevier.com/locate/biomaterials

Bioreactor-engineered cancer tissue-like structures mimic phenotypes, gene expression profiles and drug resistance patterns observed "in vivo"

Christian Hirt [a, b, 1], Adam Papadimitropoulos [a, b, 1], Manuele G. Muraro [a, b], Valentina Mele [a, b], Evangelos Panopoulos [a, b], Eleonora Cremonesi [a, b], Robert Ivanek [b], Elke Schultz-Thater [a, b], Raoul A. Droeser [a], Chantal Mengus [a, b], Michael Heberer [a, b], Daniel Oertli [a], Giandomenica Iezzi [a, b], Paul Zajac [a, b], Serenella Eppenberger-Castori [c], Luigi Tornillo [c], Luigi Terracciano [c], Ivan Martin [a, b, *], Giulio C. Spagnoli [a, b, *]

[a] Department of Surgery, University Hospital Basel, Switzerland
[b] Department of Biomedicine, University of Basel, Switzerland
[c] Institute of Pathology, University of Basel, Switzerland

ARTICLE INFO

Article history:
Received 18 February 2015
Received in revised form
8 May 2015
Accepted 18 May 2015
Available online 20 May 2015

Keywords:
Bioreactors
Tri-dimensional cultures
Tumor tissue-like structures
Colorectal cancer
Drug resistance

ABSTRACT

Anticancer compound screening on 2D cell cultures poorly predicts "in vivo" performance, while conventional 3D culture systems are usually characterized by limited cell proliferation, failing to produce tissue-like-structures (TLS) suitable for drug testing. We addressed engineering of TLS by culturing cancer cells in porous scaffolds under perfusion flow. Colorectal cancer (CRC) HT-29 cells were cultured in 2D, on collagen sponges in static conditions or in perfused bioreactors, or injected subcutaneously in immunodeficient mice. Perfused 3D (p3D) cultures resulted in significantly higher ($p < 0.0001$) cell proliferation than static 3D (s3D) cultures and yielded more homogeneous TLS, with morphology and phenotypes similar to xenografts. Transcriptome analysis revealed a high correlation between xenografts and p3D cultures, particularly for gene clusters regulating apoptotic processes and response to hypoxia. Treatment with 5-Fluorouracil (5-FU), a frequently used but often clinically ineffective chemotherapy drug, induced apoptosis, down-regulation of anti-apoptotic genes (*BCL-2*, *TRAF1*, and *c-FLIP*) and decreased cell numbers in 2D, but only "nucleolar stress" in p3D and xenografts. Conversely, BCL-2 inhibitor ABT-199 induced cytotoxic effects in p3D but not in 2D cultures. Our findings advocate the importance of perfusion flow in 3D cultures of tumor cells to efficiently mimic functional features observed "in vivo" and to test anticancer compounds.

© 2015 Elsevier Ltd. All rights reserved.

1. Introduction

Established cell lines play a central role in tumor cell biology investigations and in the development of novel anticancer treatments [1,2]. Their availability in large quantities and their relatively stable phenotypes, transcriptomes and functional characteristics represent obvious advantages. Screening of novel antitumor compounds is currently based on the assessment of their ability to inhibit proliferation or to induce cytotoxicity in human cancer cell lines cultured in high-throughput formats. Frequently however, "in vitro" behavior of established cell lines poorly mirrors "in vivo" cancer cell features [3].

Based on this background, a variety of innovative "in vitro" technologies are currently being developed to provide the scientific community with advanced models potentially overcoming limitations of current assays and eventually improving their predictive performance [4,5]. A series of studies have underlined that culture in bi-dimensional (2D) or tri-dimensional (3D) systems differentially affects sensitivity of cancer cells to compounds used in cancer treatment [6–9] or to immune effector cells specific for human tumor associated antigens [10]. These findings have been related to a variety of mechanisms, including differential drug penetration

* Corresponding authors. Department of Surgery, Basel University Hospital, ICFS, Hebelstrasse 20, 4031, Basel, Switzerland.
E-mail addresses: ivan.martin@usb.ch (I. Martin), giulio.spagnoli@usb.ch (G.C. Spagnoli).
[1] Christian Hirt and Adam Papadimitropoulos contributed equally to this article.

http://dx.doi.org/10.1016/j.biomaterials.2015.05.037
0142-9612/© 2015 Elsevier Ltd. All rights reserved.

and cell proliferation in different cell layers and modulation of defined signaling pathways, in 2D cultures and in 3D tumor-like structures.

3D cancer cell culture technologies have been suggested to mimic, at least in part, "in vivo" tumor microenvironmental conditions such as cell-to-cell contact and cell-extracellular matrix (ECM) interactions, or generation of hypoxic-necrotic areas, potentially playing a role in tumor metabolism and progression and in metastasis formation [11,12]. Alternative models, based on seeding and culture of tumor cells within porous 3D scaffolds composed of different materials with potentially tunable architectural complexity, have also been described [13,14].

Notably however, although 3D cultures may share morphological and biochemical features of "in vivo" growing tumors, they are usually characterized by poor cell proliferation and display only scattered areas of clustered tumor cells, with limited resemblance to xenografts and human malignant tissues [13,14], possibly due to mass transport limitations associated with tissue growth [15].

The use of bioreactor devices has been proposed to provide a dynamic culture environment promoting tissue viability, maturation and availability of bioactive factors, thereby supporting the generation of uniform tissue-like structures (TLS) [16]. In the context of tumor cell cultures, most bioreactor-based approaches have introduced agitation techniques and microfluidic platforms [17–19], generating hydrodynamic conditions in the form of convectional fluid flow around cells and tissues. However, resulting superficial flows in those systems are of limited effectiveness to address internal transport limitations [20], which in turn critically affect cell behavior and function as well as drug penetration [21].

Bioreactor devices applying direct perfusion were shown to provide uniform cell distribution [22], allowing the development and maintenance of uniformly viable large tissues for prolonged culture times [22,23]. Perfusion flow velocities may be regulated to control flow-induced shear stress and local oxygen distributions within 3D constructs [24]. Such systems have been utilized in a variety of applications for tissue engineering [23,25], but their potential for tumor tissue formation "in vitro" has not been explored so far.

Colorectal cancer (CRC) is the third most common malignancy worldwide both in women and men [26]. Despite major progress in the understanding of its molecular pathogenesis and the development of new therapies over the last decade, cure rates remain low [27]. In this study, we comparatively analyzed morphology, cell phenotype, proliferation rates, gene expression profiles and sensitivity to drug treatment in CRC cells growing in 2D cell cultures, in tumor TLS generated in perfusion-based bioreactors and in xenografts in immunodeficient mice. We here report that culture of CRC cells in perfused 3D (p3D) cultures results in the formation of tumor TLS characterized by high similarities with "in vivo" xenografts generated in immunodeficient mice.

2. Materials and methods

2.1. Cell lines and scaffolds

HT-29, SW480 and DLD-1 CRC cell lines and PC-3 (prostate cancer), A549 (non-small cell lung cancer) and BT474 (breast-cancer) cell lines were obtained from the American Type Culture Collection (ATCC) and authenticated by short tandem repeat (STR) DNA profiling. Cells were passaged for less than 6 months after resuscitation. HT-29 cells were maintained in McCoy's 5A medium (Sigma–Aldrich) containing 10% heat-inactivated fetal calf serum, GlutaMAX-I, and Kanamycin sulphate (all from Gibco, Life Technologies). All other cancer cell lines were cultured in RPMI-1640 (Sigma–Aldrich) containing 10% heat-inactivated fetal calf serum, 0.1% 2-β-Mercaptoethanol (Sigma–Aldrich), GlutaMAX-I, MEM non-essential aminoacids (NEAA), Sodium Pyruvate, HEPES buffer and Kanamycin sulphate. Collagen scaffolds (Ultrafoam, Avitene) obtained from Davol, were cut with 6–8 mm biopsy punches prior to cultures. A non-woven polyethylene (PET, 185 g/m^2) scaffold mesh was obtained from Norafin Industries and silk scaffolds were a gift from Dr. Sourabh Ghosh, Indian Institute of Technology, Delhi, India [28]. Prior to use, PET and silk scaffolds were autoclaved and cut by a biopsy punch.

2.2. Cell culture in 2D, and in static and perfused 3D conditions

For standard 2D cell cultures we used 75 cm^2 culture flasks or 8-well-tissue chamber slides (Becton Dickinson) and 5 × 10^5-10^6/mL cell concentrations. For static 3D (s3D) cell cultures, 6-well-plates (Becton Dickinson) were coated with 1 mL of 1.5% Agar in DMEM (Sigma–Aldrich) at least one day before use and kept at 4 °C. Static seeding was achieved by resuspending 10^6 cells in 40 μL of medium and letting them attach to scaffolds for 1 h at 37 °C. Culture medium (5 mL) was then added. For perfused 3D (p3D) cultures, we used a commercially available (Cellec Biotek AG) perfusion bioreactor system [29]. Cells (10^6) were seeded and perfused overnight at a superficial velocity of 400 μm/s. After a 24 h cell seeding phase, superficial velocity was reduced to 100 μm/s.

Cell seeding efficiency on different scaffolds was determined by analyzing DNA content in constructs harvested after overnight culture. Briefly, samples were digested with proteinase K solution (Sigma–Aldrich) for 16 h at 56 °C, as previously described [29], and DNA quantity was evaluated by CyQUANT Cell Proliferation Assay (Invitrogen) according to manufacturer's protocols. Fluorescence was measured by a Spectra-Max Gemini XS Microplate Spectrofluorometer (Molecular Devices), at 485 nm excitation and 538 nm emission wavelengths. Seeding efficiencies were calculated as percentages of the original cell input detectable in cultured constructs.

Cell proliferation was determined in constructs harvested at various time points using an MTT assay (Sigma–Aldrich), as previously described [28], and pH levels in culture supernatants were measured by standard methods.

2.3. Immunofluorescence, cytofluorimetry and immunohistochemistry

Constructs retrieved following 7 or 14 days cultures were fixed overnight in 1.5% paraformaldehyde at 4 °C and paraffin embedded (TPC15 Medite). Sections (5 μm) were deparaffinized, re-hydrated and stained with hematoxylin and eosin (H&E). Culture chamber slides used for 2D cultures were fixed with paraformaldehyde and directly stained with H&E.

Immunofluorescence analyses were performed following deparaffinization, re-hydration and antigen retrieval at 95 °C for 30 min with ready-to-use S1700 solution (DAKO). Proliferating cells were identified using a Ki67 specific rabbit monoclonal antibody (mAb) (ab27619, AbCAM) and apoptotic cells were identified using a cleaved caspase 3 specific rabbit mAb (cCl3, Asp175, rabbit mAb #9664, Cell Signaling) [30]. As secondary reagent, we used an Alexa-Fluor 488 labeled goat-anti-rabbit polyclonal antibody (A-11034, Invitrogen) at a 1:400 final dilution. Nuclei were counterstained with DAPI (Invitrogen). Histological and immunofluorescence sections were analyzed using a BX-61 microscope (Olympus).

Alternatively, for cytofluorimetric analysis, cells were extracted from scaffolds by treatment with TrypLE (Gibco, Life Technologies) for 10 min, followed by incubation in 0.3% collagenase (Worthington) for 30 min at 37 °C, as previously described [31], and

stained with Annexin V FITC/PI according to manufacturer's protocol (Becton Dickinson) or with a Ki67 specific mAb (see above). Cells were analyzed by flow cytometry (FACScalibur, BD).

Standard procedures (ABC-Elite, Vector Laboratories) were used for immunohistochemical analysis of paraffin embedded sections from TLS. Briefly, 5 μm slides were dewaxed and re-hydrated in distilled water. Endogenous peroxidase activity was blocked using 0.5% H_2O_2. Sections were treated with 10% normal goat serum (DakoCytomation) for 20 min and incubated with monoclonal mouse anti-human CDX2 (clone AMT28, 1:50, Abcam) and Cytokeratin 20 (clone Ks20.8, 1:50, DAKO) primary antibody for one hour at room temperature. Subsequently, sections were incubated with peroxidase-labelled secondary antibody (DakoCytomation) for 30 min at room temperature. For antigen visualization, sections were immersed in 3-amino-9-ethylcarbazole plus substrate-chromogen (DakoCytomation) for 30 min, and counterstained with Gill's hematoxylin.

2.4. Quantification of gene expression by quantitative real-time PCR

Total cellular RNA was extracted by using NucleoSpin RNA II kit (Macherey–Nagel) and reverse transcribed, as previously described [32]. Quantitative Real-Time PCR (qRT-PCR) assays were performed in the presence of primers and probes specific for the indicated genes (Assays-on-demand, Applied Biosystems). Normalization of gene expression was performed using GAPDH as reference gene [33].

2.5. RNA-sequencing and analysis

Purity of total cellular RNA was evaluated by a 2100 Bioanalyzer (Agilent Technologies). Non-stranded RNA libraries were prepared by using the Illumina TruSeq sample preparation kit and sequenced on Illumina HiSeq 2000 sequencer (Illumina).

Single-end RNA-seq reads (50-mers) were mapped to the human genome assembly, version hg19, with SpliceMap [34], implemented in Bioconductor's package QuasR. By using RefSeq mRNA coordinates from UCSC (genome.ucsc.edu, downloaded in January 2014) and the qCount function, we quantified gene expression as the number of reads that started within any annotated exon of a gene. Nucleotide sequences are deposited in the NCBI at GSE57961.

After quality control, we excluded from analysis a single sample from 2D cultures due to degraded RNA (reads obtained only at the end of transcripts) and poor correlation to other samples. Differentially expressed genes were identified using the edgeR package (version 3.4.2) [35]. Multidimensional scaling was used to visualize the relation between different cultures conditions. Differentially expressed genes, defined as having FDR $\leq$ 0.05 in any pairwise comparison, were clustered into 13 clusters using PAM algorithm [36]. Individual clusters were tested for enrichment in functional annotations using DAVID and REVIGO bioinformatics resources, as previously described [37,38].

2.6. "In vitro" and "in vivo" drug-sensitivity assays

Chemotherapeutic agents were used at the following concentrations in "in vitro" assays: 5-Fluoruracil (5-FU, Teva Pharma), 1 μg/ml and 10 μg/mL; Oxaliplatin (Sanofi-Aventis), 1 μg/mL and 10 μg/mL; Irinotecan (Pfizer), 10 μg/mL and 100 μg/mL; Sunitinib (LC Laboratories), 0.8 μg/mL and 8 μg/mL; ABT-199 (Active Biochemicals), 2.2 μg/mL.

"In vitro" tests were performed in standard 2D in 96 or 12 flat bottom wells trays (Falcon) following a one day pre-culture or in 3D perfused bioreactors following a four days pre-culture. In all conditions, a 10^5 cells/mL concentration was used. Effects of chemotherapeutic agents were assessed after 48 or 96 h by DNA content analysis, as described above. Flow cytometric, histological and immunofluorescence studies were performed at the same times.

"In vivo" assays were performed at Oncotest GmbH. Briefly, NMRI-mice were injected with 400′000 HT-29 cells in Matrigel (Becton Dickinson). After reaching a tumor volume of 6 mm^3, usually after 21 days, a 5-FU bolus (50 μg/kg) was administered and animals were sacrificed after 48 or 96 h. Xenografts were explanted and further analyses were performed in Basel, as for the "in vitro" conditions. In each experiment, four mice per time point and condition were used.

2.7. Statistical analysis

Data are presented as mean values ± standard deviations (SD). Statistical comparisons between groups were performed by one or two-way analysis of variance (ANOVA) followed by post-hoc Tukey or Bonferroni tests. In all cases, p values $\leq$ 0.05 were considered statistically significant. GraphPad Prism (Software Inc.) and R version 3.0.2 (http://www.R-project.org) softwares were used for statistical analysis.

3. Results

3.1. Generation of tumor tissue-like structures on 3D scaffolds in perfused bioreactors

To evaluate the possibility to engineer "in vitro" TLS, we seeded cells from established tumor cell lines onto 3D porous scaffolds located within perfused bioreactor chambers (Fig. 1A) [23,31]. In this device, cells suspensions and culture media flow directly through the pores of the 3D scaffolds, resulting in efficient and uniform cell distribution [23], and allowing the subsequent development and maintenance of a uniformly viable tissue for prolonged culture times [22]. Different types of scaffolds were initially tested (Supplementary Fig. S1A). However, PET scaffolds were difficult to process for histological analysis and silk scaffolds underwent substantial structural modifications upon perfusion. Instead, collagen scaffolds were found to be compatible with perfusion, likely because of their natural composition, fiber structure, and simplicity of histological processing and cell retrieval by using commercially available enzymes. Therefore, this material was selected and used for the rest of our study.

Since we are particularly interested in the investigation of colorectal cancer (CRC) cell biology and microenvironmental features [39–41], we addressed in detail the generation of TLS upon 3D culture of cells from established CRC cell lines in p3D. HT-29, DLD-1 and SW480 CRC cell lines could be maintained in culture for over 7 days in the bioreactor system under investigation and developed TLS (Supplementary Fig. S1B). Mismatch repair proficient HT-29 cell line, yielding high-density tissue-constructs upon p3D culture (see below), was selected for additional studies.

The p3D cultures were characterized by a clearly more homogeneous cell seeding as compared to s3D ones, and by a higher cell density, as detectable by whole scaffold MTT uptake after a 7 days culture (Fig. 1B, upper and lower panels, respectively). Growth curves of cells cultured in 2D, s3D or p3D, displayed markedly different patterns (Fig. 1C). Standard monolayers reached a plateau after 3 days, whereas cells in p3D cultures displayed a significantly slower proliferation (Fig. 1C). Remarkably however, the lowest proliferation rate was observed in s3D cultures performed by using the same collagen scaffold as in p3D. In analogy with trends published using a variety of other cell types [25], this is possibly due to mass transport limitations, resulting in decreasing nutrient and

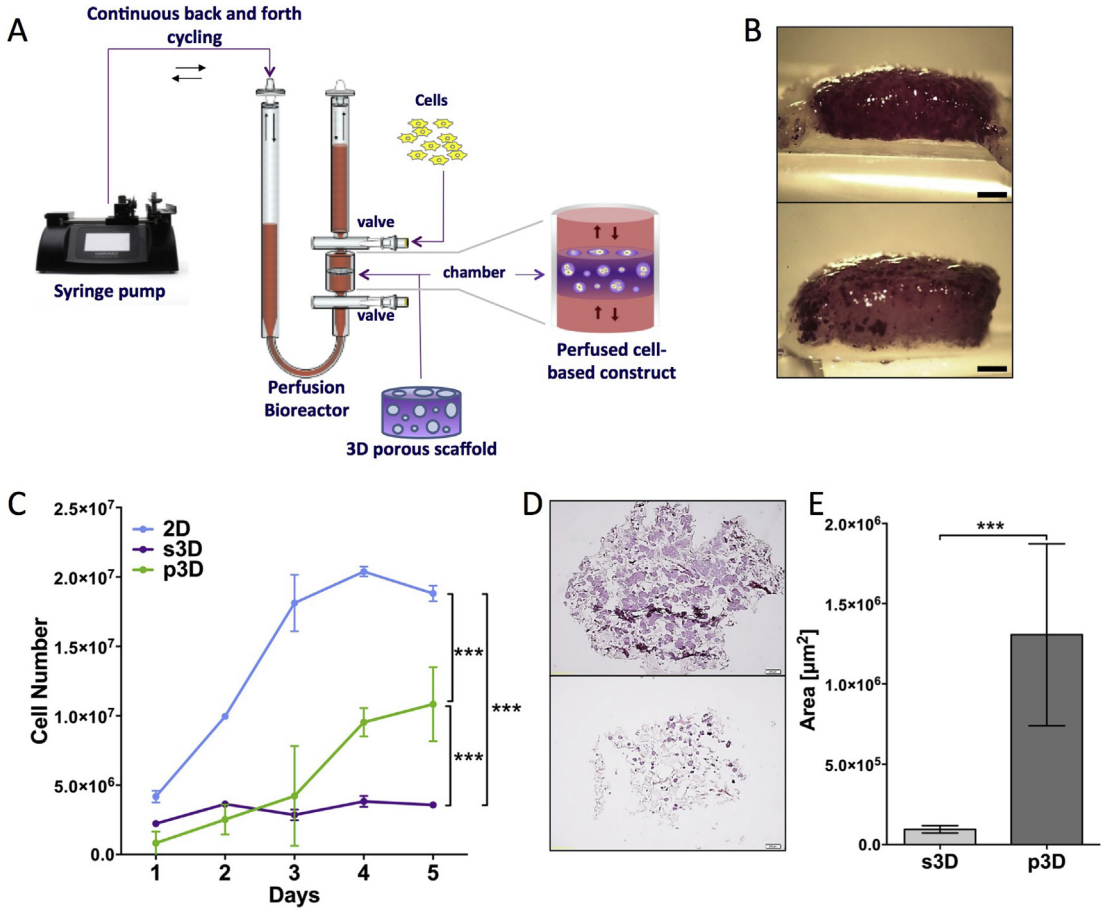

Fig. 1. Growth characteristics of perfused and static tridimensional cultures. A: A schematic view of the bioreactor utilized for the culture of tumor cells in perfused tridimensional (p3D) conditions. This device includes a perfusion chamber allocating a 3D porous scaffold. Cell suspensions or culture media may be introduced into the bioreactor through its valves. Fluid flow in alternate directions directly through the scaffold/resulting tissue is generated by using a pump connected with the bioreactor, programmed to deliver defined flow velocities. B: MTT staining of collagen scaffolds seeded with HT-29 cells in p3D (upper panel) or in s3D (lower panel) conditions, following a 7 days culture (scale bar: 1 mm). C: Proliferation kinetics of HT-29 cells under different culture conditions. D: H&E staining of whole scaffold sections from p3D (upper left panel) or s3D (lower left panel) cultures (scale bar: 200 µm). E: Histomorphometric assessment of tumor tissue areas in whole scaffold sections from s3D and p3D cultures of HT-29 cells (right panel) (***: $p < 0.001$).

oxygen availability. These growth patterns were mirrored by decreasing pH values over time (Supplementary Fig. S2).

H&E staining showed that perfusion promoted the generation of high density, homogeneous TLS (Fig. 1D, upper panel). In contrast, and consistent with previous studies [13,14], in s3D cultures small tumor areas were only detectable on the outer rims of the scaffolds while inner parts were largely free of tumor cells (Fig. 1D, lower panel). Average cross-sectional areas covered by tumor tissues in p3D cultures were over 10-fold larger than those measured in s3D conditions (Fig. 1E).

To address the broad applicability of p3D tumor cell culture, we tested a variety of cell lines of different histological origin, including PC-3 (prostate cancer), A549 (non-small cell lung cancer) and BT474 (breast cancer), in the bioreactor system under investigation. Different cell lines showed slightly different growth patterns in p3D cultures. For example, whereas HT-29 cells were growing as tumor nodules, DLD-1 cells formed tissue-like structures oriented by the scaffold-fibers. In all cases, however, p3D cultures resulted in the expansion of higher cell numbers, as compared to s3D cultures, and in the generation of larger TLS (Supplementary Fig. S3).

3.2. Histological and transcriptional profiles of p3D tumor cultures

Histological characteristics of HT-29 CRC cells cultured in monolayers and of tissue-like 3D structures generated in p3D or s3D were then evaluated in comparison with xenografts obtained "in vivo" upon subcutaneous (s.c.) injection in immunodeficient mice (Fig. 2A). HT-29 cells cultured in 2D showed homogeneous cell shape and nodular-like growth upon H&E staining. Culture in s3D conditions resulted in the generation of small tissue nodules (Fig. 2A). HT-29 cell culture in p3D conditions promoted the formation of large, anaplastic tumor TLS integrating into the collagen scaffold. Interestingly, HT-29 cells from p3D cultures and xenografts displayed a high grade of mitotic figures and atypical mitoses, as well as signet ring cells and acini-like structures (Supplementary Fig. S4A, B).

Cytokeratin 20 (CK20) was consistently expressed in all culture conditions and in xenografts, whereas CDX2 [42] was undetectable in cells from 2D cultures and expressed to different extents in HT-29 cells from s3D and p3D cultures and xenografts (Fig. 2A).

In agreement with the observed proliferation rates (Fig. 2B), Ki67 positive cells were ubiquitously detectable in monolayer cultures, rare in s3D cultures and detectable to higher extents in both p3D cultures and xenografts (Fig. 2A). Conversely, cCl3 positive, apoptotic HT-29 cells were rare in monolayer cultures, but detectable to significantly higher extents in TLS from s3D than in p3D cultures or xenografts (Fig. 2A, C).

Transcriptional profiles of cells cultured in the different

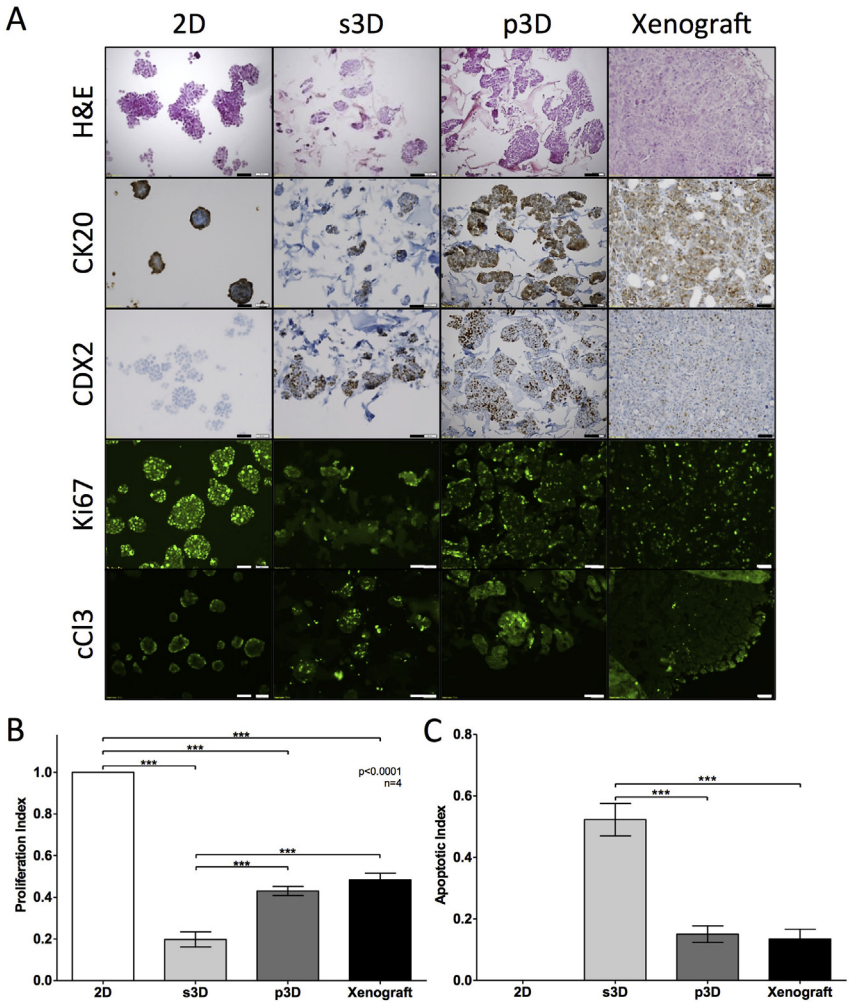

Fig. 2. Comparative analysis of phenotype and proliferation potential of HT-29 cells cultured in different conditions. A: HT-29 cells cultured in the indicated conditions or injected subcutaneously in NMRI-mice (xenografts) were stained by H&E or by Cytokeratin 20 (CK20) or CDX2 specific mAbs. Specific binding was visualized by standard immunohistochemical techniques. In parallel experiments, cells were stained by using fluorochrome labeled Ki67 and Cleaved Caspase 3 (cCl3) specific mAbs (scale bar: 50 μm). B: Proliferation index was calculated as ratio of Ki67 + cells to total cell number. C: Apoptotic index was calculated as ratio of cCl3+ cells to total cell number. (***: $p < 0.001$).

conditions under investigation and growing in xenografts were investigated by RNA sequencing. A comparative analysis revealed high similarities between all "in vitro" cultures and xenografts ($r > 0.97$). However, the expression of defined gene clusters appeared to be differentially regulated in 2D, s3D and p3D cultures and xenografts (Fig. 3). In particular, genes from cluster #2 controlling, among other functions, ribosome biogenesis and translation were highly expressed in 2D cultures. In contrast, genes from cluster #12, associated with cell cycle control and DNA transcription and repair, were expressed to higher extents in 3D cultures and xenografts, as compared to 2D cultures. On the other hand, expression of gene clusters controlling, among other processes, apoptosis and response to hypoxia (i.e., #10 and #4), was more similar to xenografts in p3D than in 2D or s3D cultures. Instead, gene clusters regulating cell adhesion and migration, as well as immune-related processes (i.e., #1 and #11), were expressed to uniquely high extents in xenografts, possibly due to the interaction with murine stromal and innate immune system cellular components "in vivo".

Taken together, these data clearly indicate that p3D culture of HT-29 CRC cells promotes the formation of relatively large tumor TLS, characterized by proliferation, and apoptotic rates as well as gene expression and phenotypic profiles similar to tumor tissues "in vivo".

3.3. Response of HT-29 p3D culture to chemotherapeutic treatment

We then explored responsiveness to current chemotherapy treatments in p3D cultures and xenografts, using, as control, currently utilized, standard 2D cultures. As s3D cultures failed to induce the generation of TLS of sizes amenable to drug testing and were characterized by negligible cell proliferation and high apoptotic rates, they were not further considered as experimental group.

We treated p3D cultured cells and xenografts with 5-Fluoruracil (5-FU), which is included in standard neo-adjuvant and adjuvant protocols for CRC treatment. For "in vitro" studies, 5-FU was used at a 1 μg/mL concentration, whereas for xenograft treatment we chose a 50 μg/kg dose, which has been reported to produce plasma levels similar to those used "in vitro" [43].

Following a 48 h treatment, signs of cellular "stress" were detectable to different extents in all cultures and in xenografts (Fig. 4A) [44]. In 2D cultures, nucleoli became prominently visible in all cells, whereas in p3D cultures and xenografts this effect was significantly reduced (Fig. 4B, left panel).

Remarkably, in 2D cultures total cell number was decreased by about 50% following a 48 or 96 h exposure to 5-FU (Fig. 4B, middle panel). In contrast, in p3D cultures and xenografts no significant

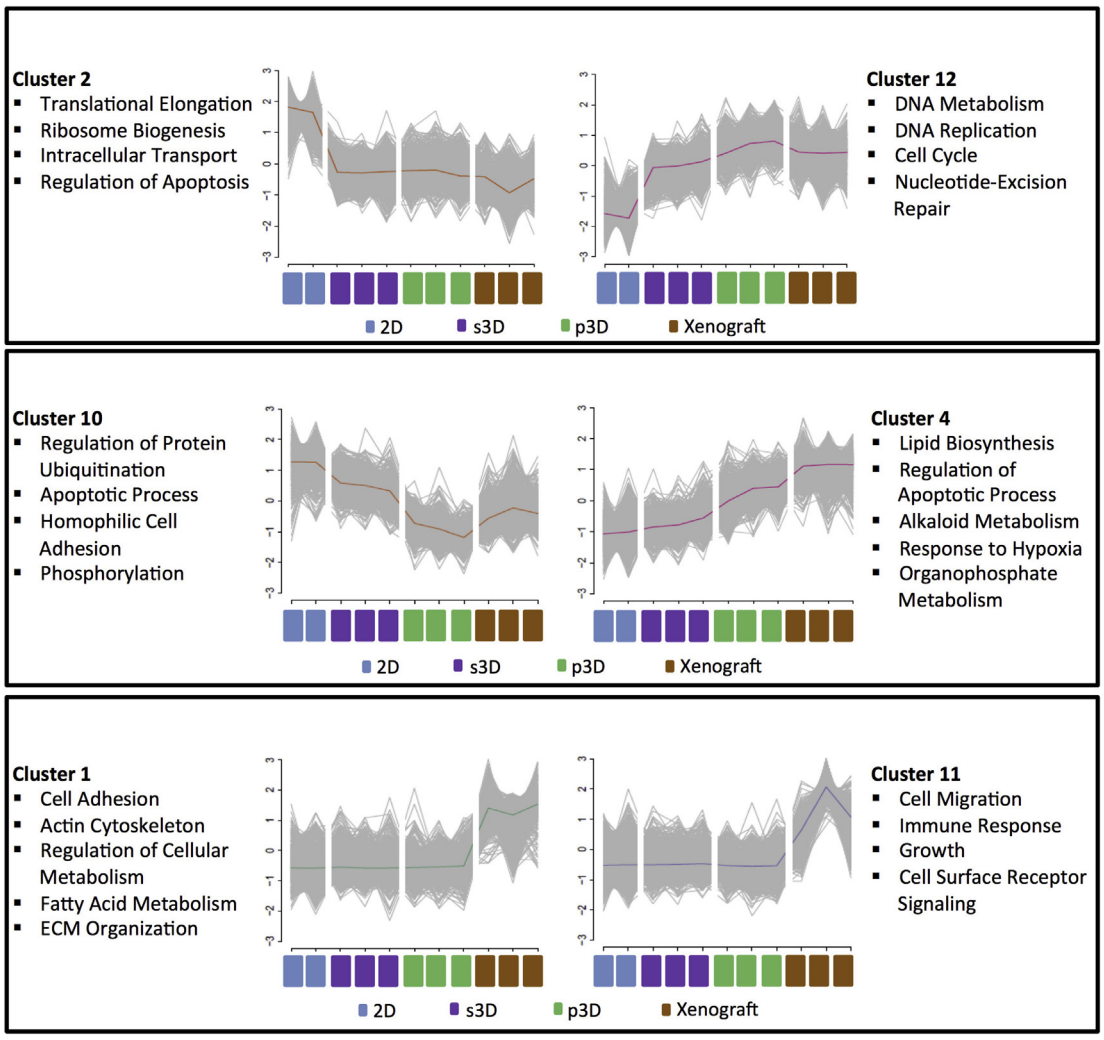

Fig. 3. Next generation sequencing transcriptome analysis of HT-29 cells cultured in 2D, s3D and p3D conditions or growing as xenografts. Total cellular RNA was extracted from cells cultured according to the indicated conditions or growing as xenografts. Expression profiles and enriched pathways in selected gene clusters were analyzed based on DAVID Functional Annotation and REVIGO using GO Biological Processes.

reduction of total cell numbers or tumor volumes could be observed (Fig. 4B). Similar trends were also observed by using other drugs commonly utilized in CRC treatment (Supplementary Fig. S5). In agreement with these data, a significant increase in apoptotic cell numbers upon treatment was observed in 2D, but not in p3D cultures or xenografts after 96 h of treatment (Fig. 4B, right panel).

To obtain a more detailed insight into the effects of 5-FU treatment on cells cultured in different conditions and in xenografts, we analyzed by qRT-PCR the expression of a large panel of genes potentially regulating defined tumor environmental features, cell cycle and apoptosis induction. Expression of PD-L1 [45] and CCL22 chemokine genes was similarly increased upon 5-FU treatment in 2D, p3D cultures and in xenografts (Supplementary Fig. S6A, B). In contrast, IL-8 gene expression was exclusively increased in 5-FU treated HT-29 cells cultured in 2D, but not in p3D cultures or xenografts (Supplementary Fig. S6C). Most importantly, the expression of genes associated to anti-apoptotic effects, such as BCL-2, TRAF-1 and c-FLIP, was significantly down regulated upon 5-FU treatment in 2D cultures (Fig. 4C). In contrast, c-FLIP and TRAF-1 gene expression was unaffected in p3D cultures or xenografts. Regarding BCL-2 expression, marginal, non-significant, decreases were observed in p3D cultures and similarly non-significant increases were detected in treated xenografts. Taken together, our data suggest that responsiveness to 5-FU treatment appears to follow similar patterns in p3D cultures and xenografts.

Based on data emerging from 5-FU treatment of HT-29 cells, we reasoned that inhibition of anti-apoptotic proteins could potentially represent a viable treatment strategy in CRC. Interestingly, a BCL-2 inhibitor (ABT-199) has recently been developed for leukemia treatment [46]. This drug had no effect on HT-29 cells cultured in 2D, whereas a significant reduction in the number of HT-29 cells cultured in p3D was detectable upon 48 h treatment (Fig. 5A). Annexin V-PI staining showed that ABT-199 treatment led to a two-fold (46.6% vs. 22.4%) increase in the percentage of HT-29 cells undergoing apoptosis, as compared to untreated or 5-FU treated cells. Accordingly, H&E staining of ABT-199 treated p3D cultures documented a marked reduction in size of HT-29 tissue-like structures (Fig. 5B).

4. Discussion

In this study we have used a perfused bioreactor system previously utilized for the culture of different mesenchymal cell types [20,31]to address the generation of TLS from established cancer cell lines and to explore their functional characteristics. We observed that p3D culture of established human tumor cell lines resulted in

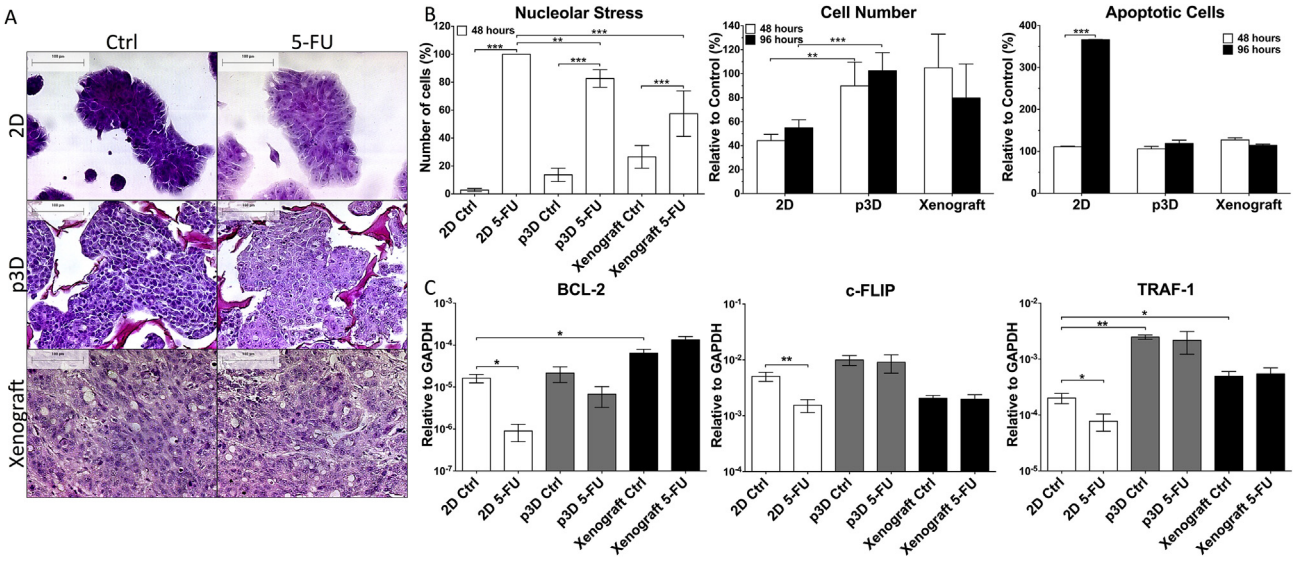

Fig. 4. Responsiveness of HT-29 cells cultured in different conditions to 5-FU treatment. A: HT-29 cells were cultured in the indicated conditions or injected subcutaneously in NMRI-mice. Cultures and experimental animals were then treated by 5-FU (1 μg/mL and 50 μg/kg, respectively), for 48 h, as detailed in "Materials and methods". Cells and tissue sections were stained by H&E according to standard methods (scale bar: 100 μm). B: Percentages of cells showing evidence of nucleolar stress in untreated cultures and animals or following a 48 h 5-FU treatment (left panel). Effects of 48 and 96 h 5-FU treatment on total tumor cell number or tumor volume as assessed by DNA staining, as compared to untreated controls (middle panel). Increases in apoptotic tumor cell percentages upon 5-FU treatment in comparison to untreated controls, as measured by Annexin V-PI staining (right panel). C: Total cellular RNA was also extracted from HT-29 cells cultured according to the indicated conditions or growing as xenografts in NMRI-mice following a 24 h treatment with 5-FU, and reverse transcribed. Expression of BCL-2 (left panel), c-FLIP (middle panel) and TRAF-1 (right panel) genes was measured by qRT-PCR, using GAPDH gene expression as reference. (*: $p < 0.05$; **: $p < 0.01$; ***: $p < 0.001$).

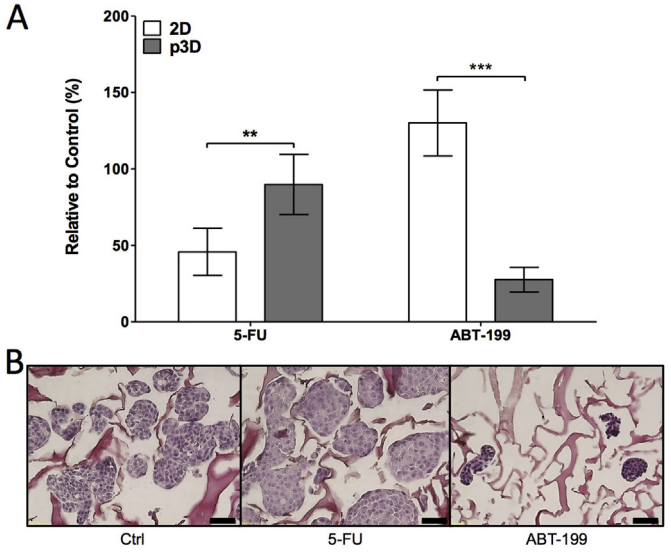

Fig. 5. Differential responsiveness to 5-FU and BCL-2 inhibition by HT-29 cells in 2D and p3D cultures. A: Effects of 48 h treatment with 5-FU or ABT-199 on total numbers of HT-29 cells cultured in 2D or in p3D cultures, as measured by DNA dye staining. B: H&E staining of p3D cultures of HT-29 cells untreated (Ctrl) or following treatment with 5-FU or ABT-199. Scale bar: 50 μm (**: $p < 0.01$; ***: $p < 0.001$).

the rapid generation of TLS characterized by more homogeneous cellular organization and significantly higher cell yields, as compared to s3D cultures. Most importantly, apoptosis, proliferation rates and response to 5-FU in p3D cultures matched those detectable in xenografts of the same cells in immunodeficient mice.

We have studied in detail the HT-29 CRC cell line. Culture of these cells in collagen sponges under perfusion flow resulted in the generation of acini-like formations, reminding histological features of differentiated colorectal mucosa. Interestingly, the formation of these structures was previously attributed to cellular polarization associated with modifications of culture medium and, possibly, related to glutamine deprivation [47]. CDX2 homeobox gene has been shown to be highly expressed in colonic adenocarcinomas, typically displaying a high intensity specific staining in 90% of cases [42]. In our study, HT-29 cells cultured in 2D did not express CDX2. However, specific staining was readily observed, to different intensities, upon culture in 3D, irrespective of perfusion, or upon injection in immunodeficient animals, thereby further supporting the notion of the high similarity between 3D cultures of established cancer cell lines and xenograft specimens.

These data prompted us to perform a comparative analysis by next generation sequencing of the whole transcriptome of HT-29 cells cultured in different conditions or growing as xenografts. This study indicates that gene expression profiles of cultured or xenografted HT29 cells are highly similar. However, defined gene clusters appeared to be differentially expressed in cells cultured in 2D, s3D, and p3D cultures or xenografts. In particular, it is remarkable that clusters of genes regulating apoptotic process and response to hypoxia appeared to be similarly expressed in p3D cultures and in xenografts. These findings might be related to the maintenance of inner tissue structures in p3D cultures and to their exposure to oxygenation gradients, thereby mimicking the presence of hypovascularized areas in "in vivo" xenografts.

We then addressed the sensitivity to drug treatment of tumor TLS generated in p3D, in comparison with xenografts, and conventional HT-29 monolayers, the current standard. While HT-29 cells in 2D cultures were highly sensitive to 5-FU treatment, p3D cultures and xenografts were similarly characterized by a partial sensitivity, as indicated by cell "stress" signs in the absence of significant cytotoxicity. These effects were accompanied by typical gene signatures. In particular, 5-FU induced BCL-2, c-FLIP and TRAF-1 gene down-regulation in treated HT-29 cell monolayers. However, the expression of these genes was not significantly affected in "stressed" HT-29 cells from treated xenografts or p3D cultures. Our

results underline that the same CRC cell line cultured in p3D and xenografts not only shares similar functional, phenotypic and gene expression profiles, but is also characterized by a similar unresponsiveness to drug treatment.

These data, concurrently underlining the major role potentially played by the expression of anti-apoptotic genes in the resistance to 5-FU treatment, have urged us to investigate the effects of newly developed anti BCL-2 pharmacological treatments. Intriguingly, ABT-199, a promising BCL-2 inhibitor currently being tested in clinical trials for chronic lymphocytic leukemia [46], did not impact on viability of HT-29 cells cultured in monolayers. In sharp contrast, ABT-199 treatment of p3D cultures led to substantial decreases in total cell numbers. Further research is warranted to clarify molecular mechanisms underlying differential sensitivity to BCL-2 inhibition in different culture systems and with additional cell lines. Nevertheless, collectively, these findings indicate that standard 2D assays not only overestimated the antitumor effectiveness of 5-FU, but dramatically underestimated the therapeutic potential of unrelated compounds [48], which was, instead, revealed by p3D cultures.

Thus, p3D cultures may represent “in vitro” models of CRC of potentially high significance in drug screening and to address drug resistance mechanisms or basic tumor biology issues under controlled conditions by taking advantage of human cells. Moreover, the p3D culture system described here may be used to efficiently mimic phenotypic and functional features observed in animal models and clinical specimens. Similar technologies could also be used to generate primary tumor cultures from clinical specimens for personalized treatment assessment.

Our study has several limitations. In particular, molecular mechanisms underlying differential phenotypic, transcriptional and functional profiles detectable in monolayers, s3D and p3D cultures are largely unclear. Furthermore, most obviously, p3D cultures fail to account for the huge complexity of cancer microenvironment and for tumor cell heterogeneity. In order to partially address the latter issues, the p3D culture system could also be extended to include the co-culture of a variety of tumor cells with additional, non-transformed cell types such as mesenchymal stromal cells, tumor-associated fibroblasts or endothelial and immunocompetent cells, in order to explore tumor specific microenvironmental features [4]. On the other hand, the use of tumor TLS generated in p3D, eventually produced in miniaturized systems [18,49], properly adapted for the application of direct perfusion, could help to overcome limitations inherent in the use of human cell lines xenografts for drug screening. This could be especially relevant regarding costs, time requirements and confounding effects of murine stromal and innate immune system cells.

Acknowledgments

Funding by the Lichtenstein-Stiftung of the University of Basel (CH) DMS2209, the Kommission für Technologie und Innovation (KTI, Bern, Switzerland) (GCS) and the Department of Surgery of the University Hospital Basel is gratefully acknowledged.

Appendix A. Supplementary data

Supplementary data related to this article can be found at http://dx.doi.org/10.1016/j.biomaterials.2015.05.037.

References

[1] M.J. Garnett, E.J. Edelman, S.J. Heidorn, et al., Systematic identification of genomic markers of drug sensitivity in cancer cells, Nature 483 (2012) 570–575.
[2] J.L. Wilding, W.F. Bodmer, Cancer cell lines for drug discovery and development, Cancer Res. 74 (2014) 2377–2384.
[3] C.H. Lieu, A.C. Tan, S. Leong, J.R. Diamond, S.G. Eckhardt, From bench to bedside: lessons learned in translating preclinical studies in cancer drug development, J. Natl. Cancer Inst. 105 (2013) 1441–1456.
[4] D.W. Hutmacher, R.E. Horch, D. Loessner, et al., Translating tissue engineering technology platforms into cancer research, J. Cell. Mol. Med. 13 (2009) 1417–1427.
[5] M. Wu, M. Swartz, Modeling tumor microenvironments in vitro, J. Biomech. Eng. (2014). BIO 13-1492.
[6] M.J. Bissell, D. Radisky, Putting tumours in context, Nat. Rev. Cancer 1 (2001) 46–54.
[7] D. Herrmann, J.R. Conway, C. Vennin, et al., Three-dimensional cancer models mimic cell-matrix interactions in the tumour microenvironment, Carcinogenesis 35 (2014) 1671–1679.
[8] R.E. Horch, A.M. Boos, Y. Quan, et al., Cancer research by means of tissue engineering—is there a rationale? J. Cell. Mol. Med. 17 (2013) 1197–1206.
[9] K.M. Yamada, E. Cukierman, Modeling tissue morphogenesis and cancer in 3D, Cell 130 (2007) 601–610.
[10] C. Feder-Mengus, S. Ghosh, A. Reschner, I. Martin, G.C. Spagnoli, New dimensions in tumor immunology: what does 3D culture reveal? Trends Mol. Med. 14 (2008) 333–340.
[11] R.A. Cairns, I.S. Harris, T.W. Mak, Regulation of cancer cell metabolism, Nat. Rev. Cancer 11 (2011) 85–95.
[12] J.A. Joyce, J.W. Pollard, Microenvironmental regulation of metastasis, Nat. Rev. Cancer 9 (2009) 239–252.
[13] C. Fischbach, R. Chen, T. Matsumoto, et al., Engineering tumors with 3D scaffolds, Nat. Methods 4 (2007) 855–860.
[14] E.L. Fong, S.E. Lamhamedi-Cherradi, E. Burdett, et al., Modeling Ewing sarcoma tumors in vitro with 3D scaffolds, Proc. Natl. Acad. Sci. U. S. A. 110 (2013) 6500–6505.
[15] S.E. Lamhamedi-Cherradi, M. Santoro, V. Ramammoorthy, et al., 3D tissue-engineered model of Ewing's sarcoma, Adv. Drug Deliv. Rev. 79–80C (2014) 155–171.
[16] D.W. Hutmacher, D. Loessner, S. Rizzi, D.L. Kaplan, D.J. Mooney, J.A. Clements, Can tissue engineering concepts advance tumor biology research? Trends Biotechnol. 28 (2010) 125–133.
[17] S. Breslin, L. O'Driscoll, Three-dimensional cell culture: the missing link in drug discovery, Drug Discov. Today 18 (2013) 240–249.
[18] Y. Wen, X. Zhang, S.T. Yang, Microplate-reader compatible perfusion microbioreactor array for modular tissue culture and cytotoxicity assays, Biotechnol. Prog. 26 (2010) 1135–1144.
[19] J.J. Winkenwerder, P.L. Palechek, J.S. Reece, et al., Evaluating prostate cancer cell culturing methods: a comparison of cell morphologies and metabolic activity, Oncol. Rep. 10 (2003) 783–789.
[20] V.I. Sikavitsas, G.N. Bancroft, A.G. Mikos, Formation of three-dimensional cell/polymer constructs for bone tissue engineering in a spinner flask and a rotating wall vessel bioreactor, J. Biomed. Mater. Res. 62 (2002) 136–148.
[21] G. Mehta, A.Y. Hsiao, M. Ingram, G.D. Luker, S. Takayama, Opportunities and challenges for use of tumor spheroids as models to test drug delivery and efficacy, J. Control Release 164 (2012) 192–204.
[22] D. Wendt, S. Stroebel, M. Jakob, G.T. John, I. Martin, Uniform tissues engineered by seeding and culturing cells in 3D scaffolds under perfusion at defined oxygen tensions, Biorheology 43 (2006) 481–488.
[23] D. Wendt, A. Marsano, M. Jakob, M. Heberer, I. Martin, Oscillating perfusion of cell suspensions through three-dimensional scaffolds enhances cell seeding efficiency and uniformity, Biotechnol. Bioeng. 84 (2003) 205–214.
[24] M. Cioffi, J. Kuffer, S. Strobel, G. Dubini, I. Martin, D. Wendt, Computational evaluation of oxygen and shear stress distributions in 3D perfusion culture systems: macro-scale and micro-structured models, J. Biomech. 41 (2008) 2918–2925.
[25] I. Martin, D. Wendt, M. Heberer, The role of bioreactors in tissue engineering, Trends Biotechnol. 22 (2004) 80–86.
[26] D.M. Parkin, F. Bray, J. Ferlay, P. Pisani, Global cancer statistics, 2002, CA Cancer J. Clin. 55 (2005) 74–108.
[27] D. Cunningham, W. Atkin, H.J. Lenz, et al., Colorectal cancer, Lancet 375 (2010) 1030–1047.
[28] M. Bhattacharjee, S. Miot, A. Gorecka, et al., Oriented lamellar silk fibrous scaffolds to drive cartilage matrix orientation: towards annulus fibrosus tissue engineering, Acta Biomater. 8 (2012) 3313–3325.
[29] N. Sadr, B.E. Pippenger, A. Scherberich, et al., Enhancing the biological performance of synthetic polymeric materials by decoration with engineered, decellularized extracellular matrix, Biomaterials 33 (2012) 5085–5093.
[30] S. Mazumder, D. Plesca, A. Almasan, Caspase-3 activation is a critical determinant of genotoxic stress-induced apoptosis, Methods Mol. Biol. 414 (2008) 13–21.
[31] A. Braccini, D. Wendt, C. Jaquiery, et al., Three-dimensional perfusion culture of human bone marrow cells and generation of osteoinductive grafts, Stem Cells 23 (2005) 1066–1072.
[32] E. Schultz-Thater, D.M. Frey, D. Margelli, et al., Whole blood assessment of antigen specific cellular immune response by real time quantitative PCR: a versatile monitoring and discovery tool, J. Transl. Med. 6 (2008) 58.
[33] K.J. Livak, T.D. Schmittgen, Analysis of relative gene expression data using real-time quantitative PCR and the 2(-Delta Delta C(T)) Method, Methods 25

(2001) 402–408.
[34] K.F. Au, H. Jiang, L. Lin, Y. Xing, W.H. Wong, Detection of splice junctions from paired-end RNA-seq data by SpliceMap, Nucleic Acids Res. 38 (2010) 4570–4578.
[35] M.D. Robinson, D.J. McCarthy, G.K. Smyth, edgeR: a Bioconductor package for differential expression analysis of digital gene expression data, Bioinformatics 26 (2010) 139–140.
[36] A.P. Reynolds, G. Richards, B. de la Iglesia, V.J. Rayward-Smith, Clustering rules: a comparison of partitioning and hierarchical clustering algorithms, J. Math. Model. Algorithms 5 (2006) 475–504.
[37] dW. Huang, B.T. Sherman, Q. Tan, et al., DAVID Bioinformatics Resources: expanded annotation database and novel algorithms to better extract biology from large gene lists, Nucleic Acids Res. 35 (2007) W169–W175.
[38] F. Supek, M. Bosnjak, N. Skunca, T. Smuc, REVIGO summarizes and visualizes long lists of gene ontology terms, PLoS One 6 (2011) e21800.
[39] R.A. Droeser, C. Hirt, C.T. Viehl, et al., Clinical impact of programmed cell death ligand 1 expression in colorectal cancer, Eur. J. Cancer 9 (2013) 2233–2342.
[40] V. Mele, M.G. Muraro, D. Calabrese, et al., Mesenchymal stromal cells induce epithelial-to-mesenchymal transition in human colorectal cancer cells through the expression of surface-bound TGF-beta, Int. J. Cancer 11 (2013) 2583–2594.
[41] C.A. Nebiker, J. Han, S. Eppenberger-Castori, et al., GM-CSF production by tumor cells Is Associated with Improved Survival in Colorectal Cancer, Clin. Cancer Res. 20 (2014) 3094–3106.
[42] C.A. Moskaluk, H. Zhang, S.M. Powell, L.A. Cerilli, G.M. Hampton, H.F. Frierson Jr., Cdx2 protein expression in normal and malignant human tissues: an immunohistochemical survey using tissue microarrays, Mod. Pathol. 16 (2003) 913–919.
[43] G. Codacci-Pisanelli, C.L. van der Wilt, H.M. Pinedo, et al., Antitumour activity, toxicity and inhibition of thymidylate synthase of prolonged administration of 5-fluorouracil in mice, Eur. J. Cancer 31A (1995) 1517–1525.
[44] S. Boulon, B.J. Westman, S. Hutten, F.M. Boisvert, A.I. Lamond, The nucleolus under stress, Mol. Cell. 40 (2010) 216–227.
[45] P. Zhang, D.M. Su, M. Liang, J. Fu, Chemopreventive agents induce programmed death-1-ligand 1 (PD-L1) surface expression in breast cancer cells and promote PD-L1-mediated T cell apoptosis, Mol. Immunol. 45 (2008) 1470–1476.
[46] A.J. Souers, J.D. Leverson, E.R. Boghaert, et al., ABT-199, a potent and selective BCL-2 inhibitor, achieves antitumor activity while sparing platelets, Nat. Med. 19 (2013) 202–208.
[47] V.M. Weaver, S. Lelievre, J.N. Lakins, et al., Beta4 integrin-dependent formation of polarized three-dimensional architecture confers resistance to apoptosis in normal and malignant mammary epithelium, Cancer Cell 2 (2002) 205–216.
[48] R.M. Phillips, M.C. Bibby, J.A. Double, A critical appraisal of the predictive value of in vitro chemosensitivity assays, J. Natl. Cancer Inst. 82 (1990) 1457–1468.
[49] S.B. Huang, S.S. Wang, C.H. Hsieh, Y.C. Lin, C.S. Lai, M.H. Wu, An integrated microfluidic cell culture system for high-throughput perfusion three-dimensional cell culture-based assays: effect of cell culture model on the results of chemosensitivity assays, Lab. Chip 13 (2013) 1133–1143.